Article

Kinetic and Thermodynamic Characterization of Co–Substrate Radical Pair Formation in Coenzyme B-Dependent Ethanolamine Ammonia-Lyase in a Cryosolvent System by Using Time-Resolved, Full-Spectrum Continuous-Wave Electron Paramagnetic Resonance Spectroscopy

Miao Wang, and Kurt Warncke

J. Am. Chem. Soc., **2008**, 130 (14), 4846-4858 • DOI: 10.1021/ja710069y

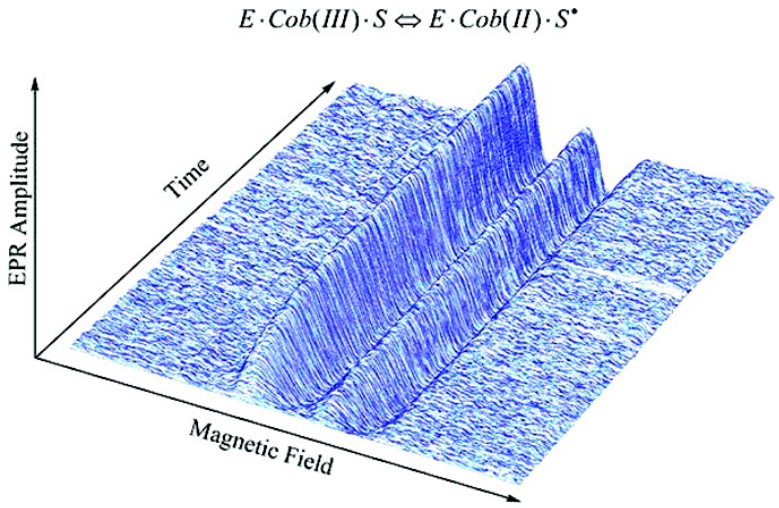

More About This Article

Additional resources and features associated with this article are available within the HTML version:

- Supporting Information
- Links to the 2 articles that cite this article, as of the time of this article download
- Access to high resolution figures
- Links to articles and content related to this article
- Copyright permission to reproduce figures and/or text from this article

View the Full Text HTML

J|A|C|S
ARTICLES
Published on Web 03/15/2008

Kinetic and Thermodynamic Characterization of Co^{II}−Substrate Radical Pair Formation in Coenzyme B_{12}-Dependent Ethanolamine Ammonia-Lyase in a Cryosolvent System by Using Time-Resolved, Full-Spectrum Continuous-Wave Electron Paramagnetic Resonance Spectroscopy

Miao Wang and Kurt Warncke*

Department of Physics, N201 Mathematics and Science Center, 400 Dowman Drive, Emory University, Atlanta, Georgia 30322-2430

Received November 6, 2007; E-mail: kwarncke@physics.emory.edu

Abstract: The formation of the Co^{II}−substrate radical pair catalytic intermediate in coenzyme B_{12} (adenosylcobalamin)-dependent ethanolamine ammonia-lyase (EAL) from *Salmonella typhimurium* has been studied by using time-resolved continuous-wave electron paramagnetic resonance (EPR) spectroscopy in a cryosolvent system. The 41% v/v DMSO/water cryosolvent allows mixing of holoenzyme and substrate, (*S*)-2-aminopropanol, at 230 K under conditions of kinetic arrest. Temperature step from 230 to 234−248 K initiates the cleavage of the cobalt−carbon bond and the monoexponential rise (rate constant, $k_{obs} = \tau_{obs}^{-1}$) of the EPR-detected Co^{II}−substrate radical pair state. The detection deadtime: τ_{obs} ratio is reduced by $>10^2$, relative to millisecond rapid mixing experiments at ambient temperatures. The EPR spectrum acquisition time is $\ll\tau_{obs}$, which allows continuous acquisition of spectra during progress of the reaction. The k_{obs} values and Co^{II}−substrate radical pair amplitudes are independent of substrate concentration at each temperature. Therefore, the reaction occurs from the enzyme·coenzyme·substrate ternary complex. The constant value of the Co^{II}−substrate radical pair amplitude at reaction times $>5\tau_{obs}$, the approximately 10^2-fold slower rate of the substrate radical rearrangement reaction relative to k_{obs}, and the reversible temperature dependence of the amplitude indicate that the Co^{II}−substrate radical pair and ternary complex are essentially at equilibrium. The reaction is thus treated as a relaxation to equilibrium by using a linear two-step, three-state mechanism. The intermediate state in this mechanism, the Co^{II}−5′-deoxyadenosyl radical pair, is not detected by EPR at signal-to-noise ratios of 10^3, which indicates that the free energy of the Co^{II}−5′-deoxyadenosyl radical pair state is >3.3 kcal/mol, relative to the Co^{II}−substrate radical pair. Van't Hoff analysis yields $\Delta H_{13} = 10.8 \pm 0.8$ kcal/mol and $\Delta S_{13} = 45 \pm 3$ cal/mol/K for the transition from the ternary complex to the Co^{II}−substrate radical pair state. The free energy difference, ΔG_{13}, is zero to within one standard deviation over the temperature range 234−248 K. The extrapolated value of ΔG_{13} at 298 K is -2.6 ± 1.2 kcal/mol. The estimated EAL protein-associated contribution to the free energy difference is $\Delta G_{EAL} = -24$ kcal/mol at 240 K, and $\Delta H_{EAL} = -13$ kcal/mol and $\Delta S_{EAL} = 38$ cal/mol/K. The results show that the EAL protein makes both strong enthalpic and entropic contributions to overcome the large, unfavorable cobalt−carbon bond dissociation energy, which biases the reaction in the forward direction of Co−C bond cleavage and Co^{II}−substrate radical pair formation.

Introduction

Radical catalysis in the coenzyme B_{12}-dependent enzymes is initiated by cleavage of the cobalt−carbon (Co−C) bond of coenzyme B_{12} (adenosylcobalamin AdoCbl; Scheme 1) to form a proposed Co^{II} (low-spin, $S = {}^1/_2$)−5′-deoxyadenosyl radical pair (step 1 of Figure 1).[1,2] The subsequent Co^{II}−radical pair separation phase of the catalytic cycle involves the migration of the C5′-methylene radical center from the β-face of cobalamin to the substrate binding site, followed by the abstraction of a hydrogen atom from the substrate to form the Co^{II}−substrate radical pair (step 2 of Figure 1; the structures of the species are shown in Scheme 2). Comparison of the rates of steady-state turnover of coenzyme B_{12}-dependent enzymes ($k_{cat} \approx 10^1-10^2$ s^{-1} at 298 K)[1,2] with the rate of cleavage of the cobalt−carbon bond of AdoCbl in solution ($k_{Co-C} = 10^{-9\pm1}$ s^{-1} at 298 K)[3] reveals that the enzymes increase the cleavage rate by $>10^{11}$-fold. Characterization of the energetics of the proposed Co^{II}−5′-deoxyadenosyl radical pair and the overall radical pair separation process is essential for understanding this remarkable rate acceleration. However, the Co^{II}−5′-deoxyadenosyl radical pair has eluded direct detection in all coenzyme B_{12}-dependent

(1) Banerjee, R. *Chemistry and Biochemistry of B12;* Wiley: New York, 1999.
(2) Brown, K. L. *Chem. Rev.* **2005**, *105*, 2075−2149.
(3) Hay, B. P.; Finke, R. G. *Polyhedron* **1988**, *7*, 1469−1481.

10.1021/ja710069y CCC: $40.75

Scheme 1

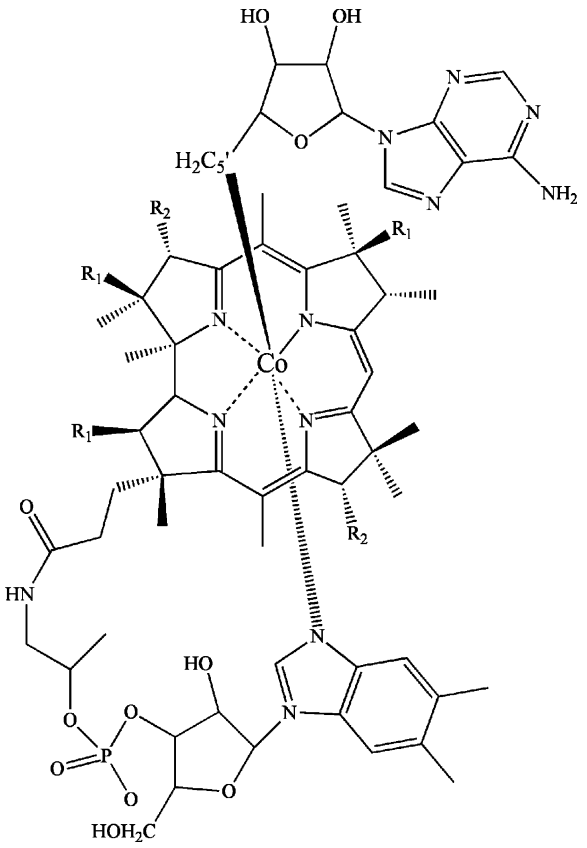

enzymes (although its existence is supported by studies of hydrogen atom exchange between the C5′ methyl center and the substrate and product carbon atoms[1,2,4]), and measurements of the thermodynamics of Co^{II}−substrate radical pair formation have not been possible, because of steady-state turnover at ambient temperature. Here, we report time-resolved measurements of the Co^{II}−substrate radical pair formation reaction by using full-spectrum, continuous-wave electron paramagnetic resonance (EPR) spectroscopy at low temperature in a cryosolvent system. The experiments are aimed at characterizing the kinetics and thermodynamics of the first two formal steps in Figure 1 in the coenzyme B_{12}-dependent ethanolamine ammonia-lyase [EAL; EC 4.3.1.7; cobalamin (vitamin B_{12})-dependent enzyme superfamily[5,6]] from *Salmonella typhimurium*.[2,7,8] EAL catalyzes the conversion of aminoethanol and (*R*)- and (*S*)-2-aminopropanols to the corresponding aldehydes and ammonia.[9]

The Co−C bond cleavage kinetics in the coenzyme B_{12}-dependent enzymes, methylmalonyl-CoA mutase, glutamate mutase, ribonucleotide triphosphate reductase, and EAL, have been studied at $T > 273$ K by using the stopped-flow method with detection of visible absorption changes associated with the adenosylcob(III)alamin ($\lambda_{max} \approx 525$ nm) to cob(II)alamin ($\lambda_{max} \approx 470$ nm) transition.[10−13] In EAL, cob(II)alamin is formed in a monoexponential process with first-order rate constants of >300 s^{-1} (mixing dead time limitation) and 74 s^{-1} following mixing of holoenzyme and the substrates, aminoethanol and (*S*)-2-aminopropanol, respectively.[13] Deuteration of the substrate leads to a decreased rate of cob(II)alamin appearance in EAL and other adenosylcobalamin-dependent enzymes.[10−13] The interpretation of this hydrogen isotope effect (in EAL, >10 and 3 for deuterated aminoethanol and (*S*)-2-aminopropanol substrates, respectively)[13] is that the Co−C bond cleavage and hydrogen atom transfer steps are kinetically coupled. The hydrogen isotope effect and prior lack of success in observing the 5′-deoxyadenosyl radical have led to consideration of two mechanisms for the radical pair separation process, as follows:[10−13] (a) The Co−C bond cleavage and Co^{II}−substrate radical pair formation reactions are concerted. (b) The Co^{II}−5′-deoxyadenosyl radical pair intermediate has a high free energy, relative to other diamagnetic and paramagnetic enzyme states. The large, 8−11 Å separation distance between cobalt and radical centers in the first metastable radical pair state in the eliminase class of coenzyme B_{12}-dependent enzymes,[14−18] which includes EAL, strongly suggests that a discrete 5′-deoxyadenosyl radical exists. This is also consistent with the small value of the electronic interaction (electron spin−spin coupling constant, J) between Co^{II} and substrate radicals of $|J| \leq 0.1$ cm^{-1}, which is equivalent to $\leq 10^{-3}$ kcal/mol, in the eliminase enzymes.

The thermodynamics of the Co−C bond cleavage has been investigated in AdoCbl-dependent ribonucleotide triphosphate reductase (RTPR) by using stopped-flow and optical detection of $Co^{III} \leftrightarrow Co^{II}$ absorbance changes.[19,20] This is possible, because RTPR has the unique ability among coenzyme B_{12}-dependent enzymes to cleave the Co−C bond in the absence of bound substrate, through interaction of the enzyme with a deoxynucleotide triphosphate activator.[21] The free energy change for the equilibrium between dGTP-activated holoenzyme and the first metastable state, a Co^{II}−thiyl radical pair, was approximately zero under pseudo-first-order conditions for AdoCbl binding.[12] Comparison with the free energy of ∼30 kcal/mol for the Co−C cleavage reaction in solution[22−24] showed that the protein significantly perturbs the equilibrium toward Co−C bond cleavage. In particular, large, favorable entropy contributions to the free energy were observed. Interpretation of the kinetics of cob(II)alamin formation in RTPR[11] and in methylmalonyl-CoA mutase[24] by using a single-step concerted mechanism for Co−C bond cleavage and radical pair formation showed that

(4) *B12;* Dolphin, D., Ed.; Wiley: New York, 1982; Vol. 2.
(5) Hubbard, T. J. P.; Ailey, B.; Brenner, S. E.; Murzin, A. G.; Chothia, C. *Nucleic Acids Res.* **1999**, *27*, 254−256.
(6) Sun, L.; Warncke, K. *Proteins: Struct., Funct., Bioinf.* **2006**, *64*, 308−319.
(7) Bandarian, V.; Reed, G. H. In *Chemistry and Biochemistry of B12;* Banerjee, R., Ed.; Wiley and Sons: New York, 1999; pp 811−833.
(8) Toraya, T. *Chem. Rev.* **2003**, *103*, 2095−2127.
(9) Bradbeer, C. *J. Biol. Chem.* **1965**, *240*, 4669−4674.
(10) Padmakumar, R.; Padmakumar, R.; Banerjee, R. *Biochemistry* **1997**, *36*, 3713−3718.
(11) Marsh, E. N. G.; Ballou, D. P. *Biochemistry* **1998**, *37*, 11864−11872.
(12) Licht, S. S.; Booker, S.; Stubbe, J. *Biochemistry* **1999**, *38*, 1221−1233.
(13) Bandarian, V.; Reed, G. H. *Biochemistry* **2000**, *39*, 12069−12075.
(14) Boas, J. F.; Hicks, P. R.; Pilbrow, J. R.; Smith, T. D. *J. Chem. Soc., Faraday Trans. 2* **1978**, *74*, 417−431.
(15) Gerfen, G. J.; Licht, S.; Willems, J. P.; Hoffman, B. M.; Stubbe, J. *J. Am. Chem. Soc.* **1996**, *118*, 8192−8197.
(16) Licht, S.; Gerfen, G. J.; Stubbe, J. *Science* **1996**, *271*, 477−481.
(17) Canfield, J. M.; Warncke, K. *J. Phys. Chem. B* **2002**, *106*, 8831−8841.
(18) Bandarian, V.; Reed, G. H. *Biochemistry* **2002**, *41*, 8580−8588.
(19) Licht, S.; Lawrence, C. C.; Stubbe, J. *Biochemistry* **1999**, *38*, 1234−1242.
(20) Brown, K. L.; Cheng, S.; Marques, H. M. *Inorg. Chem.* **1995**, *35*, 217−222.
(21) Stubbe, J.; van der Donk, W. A. *Chem. Rev.* **1998**, *98*, 705−762.
(22) Finke, R. G.; Hay, B. P. *Inorg. Chem.* **1984**, *23*, 3041−3043.
(23) Halpern, J.; Kim, S.-H.; Leung, T. W. *J. Am. Chem. Soc.* **1984**, *106*, 8317−8319.
(24) Hay, B. P.; Finke, R. G. *J. Am. Chem. Soc.* **1986**, *108*, 4820−4829.

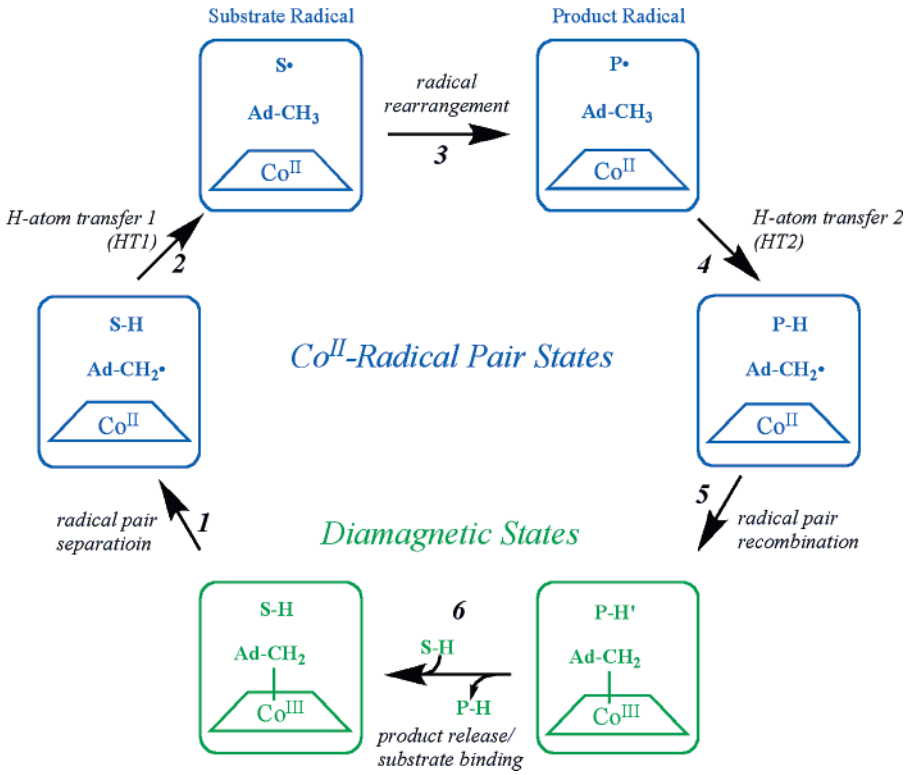

Figure 1. Minimal mechanism of catalysis for vitamin B_{12} coenzyme-dependent EAL.[7,8] The paramagnetic radical pair states and diamagnetic states are indicated. The forward direction of reaction is indicated by arrows. The structures of the reactant species are shown in Scheme 2. For the substrate, (*S*)-2-aminopropanol **1**, the cycle is reversible.[43,58,59] The steps are: (1) radical pair separation, (2) first hydrogen atom transfer (HT1), (3) radical rearrangement, (4) second hydrogen atom transfer (HT2), (5) radical pair recombination, and (6) product release/substrate binding. Substrate-derived species are designated S−H (bound substrate, **1**), S• (substrate radical, **2**), P• (product radical, **3**), and PH (diamagnetic products, aldehyde **4** and ammonia). The 5′-deoxyadenosyl β-axial ligand is represented as Ad-CH_{2-} in the intact coenzyme, and as Ad-CH_2• (5′-deoxyadenosyl radical) or Ad-CH_3 (5′-deoxyadenosine) following cobalt−carbon bond cleavage. The cobalt ion and its formal oxidation states are depicted, but the corrin ring and dimethylbenzimidazole α-axial ligand of the coenzyme[60,61] are not shown for clarity.

Scheme 2

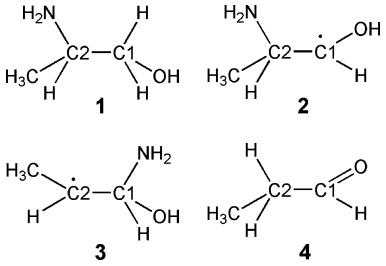

the protein also lowers the activation free energy for Co−C bond cleavage.

The rapid mixing experiments utilize sensitive visible absorption detection of $Co^{III} \leftrightarrow Co^{II}$ transitions on the millisecond time scale, but do not detect organic radicals or distinguish different paramagnetic states. EPR spectroscopy can detect and distinguish different Co^{II}−radical pair intermediates, but the time required for acquisition of the relatively broad EPR line shapes (~150.0 G for the radical pair) is $\sim 10^2$-fold greater than the rise time for Co^{II}−substrate radical pair formation at $T > 273$ K in aqueous solution. Therefore, we have developed a cryosolvent system for measurement of the radical pair formation reactions in EAL at low temperatures, to satisfy the following criteria: (a) mixing of holoenzyme and substrate [(*S*)-2-aminopropanol] under conditions of kinetic arrest of the reaction, (b) decreased rate of reaction following temperature-step initiation, to allow continuous acquisition of EPR spectra during progress of the reaction, and (c) reduction of the dead time/reaction time ratio by $>10^2$, relative to millisecond rapid mixing experiments at ambient temperatures. A binary dimethylsulfoxide (DMSO)/water cryosolvent[25,26] was chosen, because the DMSO/water system displays a low freezing point (approaching 200 K, depending upon cooling rate) and relatively high fluidity at volume percentages of 40−50% for $T \geq 230$ K.[25] DMSO/water solvent systems are commonly used in the preservation of cells, tissues, and organs during freezing and low-temperature storage.[27]

We have examined the reaction of the EAL holoenzyme with substrate (*S*)-2-aminopropanol to form the Co^{II}−substrate radical pair in EAL by using time-resolved, full-spectrum EPR spectroscopy at 234−248 K in 41% v/v DMSO/ water cryosolvent, following a temperature step from a mixing temperature of 230 K. The EPR line shape and the temperature-extrapolated first-order reaction rate constant in the cryosolvent are identical to those of EAL in aqueous solution at ambient temperatures, indicating that native structural and functional properties of the enzyme are maintained in the cryosolvent system at low temperature. The reaction is treated as a relaxation of the enzyme•coenzyme•substrate ternary complex to equilibrium with

(25) Douzou, P. *Cryobiochemistry: An Introduction;* Academic Press: New York, 1977.
(26) Travers, F.; Bertrand, R.; Roseau, G.; Vanthoai, N. *Eur. J. Biochem.* **1978**, *88*, 523−528.
(27) Lakey, J. R. T.; Anderson, T. J.; Rajotte, R. V. *Transplantation* **2001**, *72*, 1005−1011.

the Co^{II}−substrate radical pair, through an explicit Co^{II}−5′-deoxyadenosyl radical pair intermediate state, by using a linear two-step, three-state mechanism. The Co^{II}−5′-deoxyadenosyl radical is not detected. However, the first inclusion of the Co^{II}−5′-deoxyadenosyl radical pair in a kinetic mechanism for the radical pair reactions leads to a lower limit on the relative free energy of the proposed intermediate. Thermodynamic parameters for the equilibrium between the ternary complex and the Co^{II}−substrate radical pair provide insight into the contributions of the protein to Co^{II}−radical pair separation and stabilization.

Materials and Methods

Materials. All chemicals were obtained from commercial sources (Sigma-Aldrich or Fisher) and used without further purification. Enzyme was purified from the *Escherichia coli* overexpression strain incorporating the cloned *S. typhimurium* EAL coding sequences[28] essentially as described.[29]

Cryosolvent and Buffer. Several organic solvents are commonly used in cryoenzymology studies because of their low viscosity and relatively low dielectric constant of mixtures with water.[25] Among them are ethylene glycol,[26,30,31] methanol,[31,32] and DMSO.[33,34] However, ethylene glycol and methanol inactivate the EAL holoenzyme,[35,36] and ethylene glycol is too viscous for reproducible mixing at the low temperatures ($T \leq 230$ K) required to kinetically arrest the Co^{II}−substrate radical pair formation reaction. Therefore, we chose DMSO as the cryosolvent. EAL possesses a broad pH optimum from 6.6 to 8.2.[37] The standard potassium (or sodium) phosphate buffer (pH = 7.5) used in EAL studies is not appropriate for low-temperature cryoenzymology study, because of the relatively large temperature dependence of the pK_a values of phosphate.[25] Potassium cacodylate buffer, which is similar to the sodium cacodylate buffers used for cryoenzymology studies,[25] has a relatively small dependence of pK_a on temperature and was introduced for electron microscopy applications.[38] Therefore, potassium cacodylate was employed as the pH buffer. The effective pH value in the presence of DMSO was adjusted to be 7.5 ± 0.4 in the 230−273 K region. The pH values at $T < 273$ K were obtained by extrapolation of the linear dependence of pH on temperature from 298 to 273 K, as described,[25] by using a pH electrode (Corning 476156).

Sample Preparation Procedure. A 1.5-fold excess of adenosylcobalamin relative to EAL active sites was introduced into buffered (10 mM potassium cacodylate, pH = 7.1) aqueous EAL apoenzyme solution to form the holoenzyme at ambient temperature. Each EAL molecule contains six active sites.[39,40] To avoid pH and dielectric constant shock, small volumes of 70% (v/v) DMSO/water solvent (less than 15% of the volume of the holoenzyme-containing solution) were added with continuous slow mixing in four steps at decreasing temperatures over the range from 273 to 240 K, to achieve a final 41% (v/v) DMSO/water solution with holoenzyme. In the last step, the substrate, (*S*)-2-aminopropanol, in 41% (v/v) DMSO/water cryosolvent was introduced at 230 K. At this temperature, the system maintains the liquid phase. The whole system was relaxed for 5 min at 230 K to allow the substrate molecules to bind to the active site. All the procedures were performed under a dim red safe light.

Time-Resolved EPR Spectroscopy. X-band CW-EPR experiments were carried out on a Bruker ELEXSYS E500 EPR spectrometer with an ER 4123SHQE X-band cavity resonator and a Bruker ER 4131VT temperature control system. The cryostat/controller system provided a temperature stability of ±0.2 K over the length of the EPR sample cavity, as measured by using a thermocouple probe that was translated along the EPR tube axis to achieve different heights within a solution sample. All of the temperature readings in the EPR experiments were measured by using an Oxford Instruments ITC503 temperature controller with a calibrated model 19180 4-wire RTD probe, which has ±0.3 K accuracy in the 230 to 273 K region. The total temperature error of the measurements was thus estimated to be ±0.4 K.

The enzyme reaction was monitored by X-band EPR in liquid-phase samples. Therefore, capillary tubes were used to partially overcome the microwave absorption and consequent decrease in cavity quality factor (Q) caused by the lossy liquid samples. A protocol was developed to seal a 50-μL volume of substrate-bound holoenzyme from a batch sample volume of 300 μL into a 2-mm outer diameter capillary tube (Wilmad/Lab Glass, 712-SQ-250 M) at 230 K. The capillary tube was quickly transferred to the EPR cavity, which was precooled to 230 K, with the protection of cold isopentane maintained at the same temperature.

The reaction of the holoenzyme−substrate mixture was triggered by a rapid temperature step from 230 K to the desired higher temperature (234−248 K). The dead time of the system, including the temperature increase and equilibrating process (≤10 s) and microwave bridge autocalibration ("auto-tune" mode) at the high temperature set point (~10 s), was ≤20 s.

EPR Spectroscopy at 6 K. X-band CW-EPR spectroscopy at 6 K was performed by using the same Bruker ELEXSYS E500 EPR spectrometer and ER 4123SHQE X-band resonator, with an Oxford Instruments ESR-900 continuous-flow liquid helium cryostat and Oxford 3120 temperature controller. A DMSO/water cryosolvent sample, which contained EAL holoenzyme and substrate, was prepared as described in the previous section. The sample was made anaerobic by using the freeze−vacuum−thaw sequence and backfill with argon gas.

Equilibrium Perturbation Experiments. A 300-μL sample in a 4-mm outer diameter EPR tube (6-fold larger volume relative to the capillary samples) with 100-fold excess of substrate compared to EAL active sites was used in the equilibrium perturbation experiments to increase the number of detected spins, which increases the signal-to-noise ratio (SNR). The EPR instrumentation used was the same as described for the time-resolved experiments. In a typical experiment, the sample was initially adjusted to the incubation temperature, T_{inc}, in the ER 4123SHQE X-band resonator. The sample was then incubated to achieve a constant amplitude of the Co^{II}−substrate radical pair EPR signal. The incubation time period was generally $>3\tau_{obs}$, where τ_{obs} is the characteristic reaction time at T_{inc}, as determined in the time-resolved experiments and defined in eq 2. The temperature of the sample was then quickly (within 15 s) decreased to 120 K. The temperature transition time is significantly shorter than the equilibration time (15 s $\ll \tau_{obs}$). The EPR spectrum was then acquired at 120 K to retrieve the EPR signal amplitude for the substrate radical at equilibrium state, denoted as $A_{pt}(\infty, T_{inc})$. The EPR signal amplitude was measured as the difference in amplitude between the lowest field peak and highest field trough of the substrate radical line shape. The point corresponding to the maximum or minimum amplitude was identified and averaged with the adjacent two points (five points total) to obtain the recorded amplitude. The sample temperature was then stepped to the next temperature incubation set point, and the incubation and measurement process was repeated. After all desired incubation temperatures were finished, the sample temperature was raised stepwise to 273 K, to avoid sudden pH change and dielectric shock, and held for 5 min. This led

(28) Faust, L. R. P.; Connor, J. A.; Roof, D. M.; Hoch, J. A.; Babior, B. M. *J. Biol. Chem.* **1990**, *265*, 12462−12466.
(29) Faust, L. P.; Babior, B. M. *Arch. Biochem. Biophys.* **1992**, *294*, 50−54.
(30) Tesi, C.; Travers, F.; Barman, T. *Biochemistry* **1990**, *29*, 1846−1852.
(31) Bicknell, R.; Waley, S. G. *Biochemistry* **1985**, *24*, 6876−6887.
(32) Feig, A. L.; Ammons, G. E.; Uhlenbeck, O. C. *RNA* **1998**, *4*, 1251−1258.
(33) Douzou, P.; Sireix, R.; Travers, F. *Proc. Natl. Acad. Sci. U.S.A.* **1970**, *66*, 787−792.
(34) Mustafi, D.; Hofer, J. E.; Huang, W.; Palzkill, T.; Makinen, M. W. *Spectrochim. Acta, Part A* **2004**, *60*, 1279−1289.
(35) Babior, B. M. *J. Biol. Chem.* **1970**, *245*, 1755−1766.
(36) Babior, B. M.; Krouwer, J. S. *CRC Crit. Rev. Biochem.* **1979**, *6*, 35−102.
(37) Babior, B. M. In *B12;* Dolphin, D., Ed.; Wiley: New York, 1982; Vol. 2, pp 263−387.
(38) Sabatinni, D. D.; Barnett, R. J.; Bensch, K. G. *Anat. Rec.* **1962**, *142*, 274.
(39) Hollaway, M. R.; Johnson, A. W.; Lappert, M. F.; Wallis, O. C. *Eur. J. Biochem.* **1980**, *111*, 177−188.
(40) Bandarian, V.; Reed, G. H. *Biochemistry* **1999**, *38*, 12394−12402.

Scheme 3

$$A_1 \underset{k_{21}}{\overset{k_{12}}{\rightleftharpoons}} A_2 \underset{k_{32}}{\overset{k_{23}}{\rightleftharpoons}} A_3$$

to the formation of the Co^{II}−substrate radical pair in 100% of the functional EAL active sites, as found previously.[41] The fraction of EAL active sites occupied by the Co^{II}−substrate radical pair, υ_{inc}, was computed for each incubation temperature, T_{inc}, by using the following expression:

$$\upsilon_{inc}(T_{inc}) = \frac{A_{pt}(\infty,T_{inc})}{A_{pt}(\infty,T = 273\ \mathrm{K})} \quad (1)$$

Kinetic Data Fitting. It was found that the time-dependence of the substrate radical EPR signal following the temperature step was well-fit by a single-exponential growth function, as follows:

$$A_{pt}(t) = A_{pt}(\infty)[1 - e^{-k_{obs}t}] \quad (2)$$

where $A_{pt}(t)$ and $A_{pt}(\infty)$ are the time-dependent amplitude and equilibrium amplitude, respectively, measured from the lowest field peak to the highest field trough of the substrate radical EPR signal, and k_{obs} is the observed first-order rate constant for the growth of the substrate radical EPR signal. The curve fitting was performed by using the program OriginPro 7.5 (OriginLab Corporation), with the least-squares fitting method.

Mechanism for the Co^{II}−Substrate Radical Pair Formation Reaction. The measured kinetics were analyzed by using the linear two-step, three-state mechanism shown in Scheme 3. The coupled differential equations that describe the time dependence of the states in the linear two-step model presented in Scheme 3 can be solved to give analytical expressions for the normalized amplitudes of the states A_i and the relaxation rate parameters λ_i, for the initial state (at $t = 0$), $([A_1]_0/[A_1]_0) = 1$, $([A_2]_0/[A_1]_0) = ([A_3]_0/[A_1]_0) = 0$.[42] As described in the Results, this is the case for the reaction of the enzyme·coenzyme·substrate ternary complex to form the Co^{II}−substrate radical pair. The following expressions give the time dependence of the normalized amplitudes of the states A_i:[42]

$$\frac{[A_1]_t}{[A_1]_0} = \frac{k_{21}k_{32}}{\lambda_2\lambda_3} + \frac{k_{12}(\lambda_2 - k_{23} - k_{32})}{\lambda_2(\lambda_2 - \lambda_3)} e^{-\lambda_2 t} + \frac{k_{12}(k_{23} + k_{32} - \lambda_3)}{\lambda_3(\lambda_2 - \lambda_3)} e^{-\lambda_3 t} \quad (3)$$

$$\frac{[A_2]_t}{[A_1]_0} = \frac{k_{12}k_{32}}{\lambda_2\lambda_3} + \frac{k_{12}(k_{32} - \lambda_2)}{\lambda_2(\lambda_2 - \lambda_3)} e^{-\lambda_2 t} + \frac{k_{12}(\lambda_3 - k_{32})}{\lambda_3(\lambda_2 - \lambda_3)} e^{-\lambda_3 t} \quad (4)$$

$$\frac{[A_3]_t}{[A_1]_0} = \frac{k_{12}k_{23}}{\lambda_2\lambda_3} + \frac{k_{12}k_{23}}{\lambda_2(\lambda_2 - \lambda_3)} e^{-\lambda_2 t} - \frac{k_{12}k_{23}}{\lambda_3(\lambda_2 - \lambda_3)} e^{-\lambda_3 t} \quad (5)$$

The k_{ij} are defined in Scheme 3. The relaxation rate parameters, λ_i, are related to the microscopic rate constants by the following expressions:

$$\lambda_2 = \frac{1}{2}\{k_{12} + k_{21} + k_{23} + k_{32} + [(k_{12} + k_{21} + k_{23} + k_{32})^2 - 4(k_{12}k_{23} + k_{21}k_{32} + k_{12}k_{32})]^{(1/2)}\} \quad (6)$$

$$\lambda_3 = \frac{1}{2}\{k_{12} + k_{21} + k_{23} + k_{32} - [(k_{12} + k_{21} + k_{23} + k_{32})^2 - 4(k_{12}k_{23} + k_{21}k_{32} + k_{12}k_{32})]^{(1/2)}\} \quad (7)$$

and $\lambda_1 = 0$.[42]

Certain relations among the A_i are used in the analysis of the experimental data. The conservation condition is expressed in terms of the equilibrium ($t \rightarrow \infty$) concentrations of the A_i, as follows:

$$[A_1]_0 = [A_1]_\infty + [A_2]_\infty + [A_3]_\infty \quad (8)$$

The concentration of the intermediate, A_2, relative to the experimentally observed state, A_3, at equilibrium is obtained from eqs 4 and 5 for the condition, $t \rightarrow \infty$, as follows:

$$\frac{[A_2]_\infty}{[A_3]_\infty} = \frac{k_{32}}{k_{23}} = {K_{23}}^{-1} \quad (9)$$

where K_{23} is the equilibrium constant for step 2 in Scheme 3. The relative concentration of A_1 and A_3 at equilibrium is obtained from eqs 3 and 5, as follows:

$$\frac{[A_3]_\infty}{[A_1]_\infty} = \frac{k_{12}k_{23}}{k_{21}k_{32}} = K_{12}K_{23} = K_{13} \quad (10)$$

where $K_{12} = (k_{12})/(k_{21})$ is the equilibrium constant for step 1 in Scheme 3. The ratio of the concentration of the observed state at equilibrium, $[A_3]_\infty$, to the total concentration of A_i states ($[A_{tot}] = [A_1]_0$, from eq 8) is denoted as υ and is given by eq 5 in the limit $t \rightarrow \infty$, as follows:

$$\upsilon = \frac{[A_3]_\infty}{[A_1]_0} = \frac{k_{12}k_{23}}{\lambda_2\lambda_3} \quad (11)$$

Temperature Dependence of the First-Order Rate and Equilibrium Constants. The temperature dependence of the first-order rate constant, k, is given by the Arrhenius expression:[42]

$$k(T) = A\, e^{(-E_a/RT)} \quad (12)$$

where E_a is the activation energy, R is the gas constant, and A is a prefactor that represents the value of k as $E_a \rightarrow 0$. The value of A is typically approximated as (k_BT/h), where k_B is Boltzmann's constant and h is Planck's constant.

The temperature dependence of the equilibrium constant, K, is described as follows:[42]

$$K(T) = e^{(-\Delta G/RT)} = e^{(\Delta S/R)}\, e^{-(\Delta H/RT)} \quad (13)$$

where ΔG, ΔH, and ΔS are the equilibrium free energy, enthalpy, and entropy, respectively. Equation 13 is the basis for determining the ΔH and ΔS contributions to ΔG by using the van't Hoff analysis.

Results

EPR Line Shape of the Co^{II}−Substrate Radical Pair in Aqueous and Cryosolvent Systems. Figure 2 shows a representative X-band EPR spectrum, recorded at 120 K, of the Co^{II}−substrate radical pair in aqueous solution, which was prepared by the standard method of manual mixing of substrate and holoenzyme at 275 K,[17] followed by a 5-min incubation before cryotrapping at 77 K. The EPR line shape is characteristic of

(41) Hollaway, M. R.; White, H. A.; Joblin, K. N.; Johnson, A. W.; Lappert, M. F.; Wallis, O. C. *Eur. J. Biochem.* **1978**, *82*, 143−154.
(42) Moore, J. W.; Pearson, R. G. *Kinetics and Mechanism;* Wiley & Sons: New York, 1981.

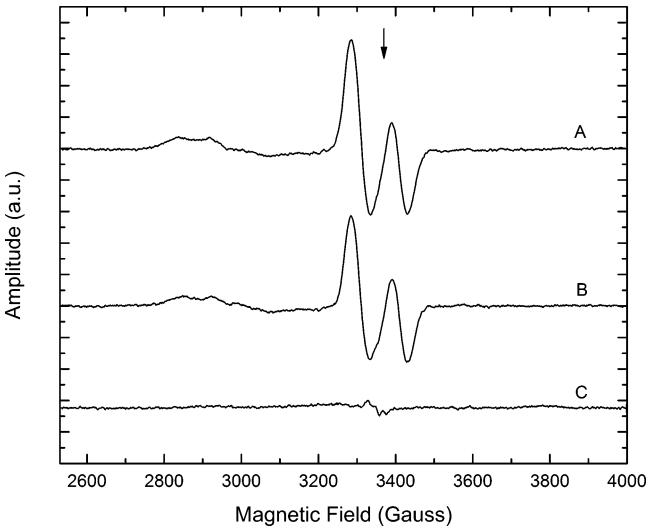

Figure 2. X-band continuous-wave EPR spectra of cryotrapped holo-EAL and substrate (*S*)-2-aminopropanol mixtures under different conditions of solvent and temperature. EPR spectroscopy was performed at $T = 120$ K. The concentrations of EAL active sites and coenzyme B_{12} were 120 μM and 12 mM, respectively. The free electron resonance position at $g = 2.0$ is shown by the arrow. (A) EPR spectrum of the Co^{II}−substrate radical pair state in aqueous solution. Holo-EAL was mixed with substrate at 275 K and then incubated on ice (273 K) for 5 min, before cryotrapping. (B) EPR spectrum of the Co^{II}−substrate radical pair state in 41% v/v DMSO/water cryosolvent. Holo-EAL was mixed with substrate at 230 K and then incubated at 273 for 5 min, before cryotrapping. (C) EPR spectrum of holo-EAL and substrate after mixing and incubation for 5 min at 230 K. EPR conditions: microwave frequency, 9.436 GHz; microwave power, 10 dB (20 mW); magnetic field modulation, 10 G peak−peak; modulation frequency, 100 kHz; field sweep rate, 1.5 G s^{-1}; time constant, 200 ms; average of two sweeps, minus average of two baseline spectra.

the (*S*)-2-aminopropanol-derived Co^{II}−substrate radical pair.[43] The Co^{II} intensity is most prominent in the region around 2850 G, which is near the $g_\perp = 2.26$ position in the EPR spectrum of magnetically isolated cob(II)alamin.[44] The substrate radical line shape extends from approximately 3250 to 3450 G. The partially resolved doublet splitting and broadening in the substrate radical line shape are caused by the interaction of the unpaired electron spin at C1 of the substrate radical with the unpaired electron spin on Co^{II}.[14,17,18]

The middle spectrum in Figure 2 shows the 120 K EPR spectrum of the Co^{II}−substrate radical pair formed in EAL in 41% v/v buffered DMSO/water cryosolvent. The cryosolvent sample was prepared by mixing holoenzyme and (*S*)-2-aminopropanol at 230 K (as described in Materials and Methods), followed by temperature increase to 273 K and incubation for 5 min before cryotrapping at 77 K. Comparison of the Co^{II}−substrate radical pair EPR spectra of the cryosolvent sample and the aqueous sample in Figure 2 shows that the line shapes are essentially identical, as also demonstrated by the overlaid, rescaled EPR spectra in Figure S1, Supporting Information. The line shape match indicates that the radical species in the cryosolvent corresponds to the substrate radical, and not the product radical. Orientation-selection pulsed-EPR studies in ethanolamine ammonia-lyase[45] and X-ray crystallographic studies of the coenzyme B_{12}-dependent diol dehydratase enzyme,[46] with which ethanolamine ammonia-lyase is mechanistically[8] and structurally[6] similar, show that the Co^{II}−C1 and Co^{II}−C2 distances are not equal, which would lead to different EPR line shapes for the substrate radical and product radical.[14,17,18] The absence of a detectable product radical species is consistent with computational studies, which predict that the energy of the product radical is 5−9 kcal/mol greater than the energy of the substrate radical.[47−49] The decrease in the amplitude of the signal in the cryosolvent sample relative to the aqueous sample in Figure 2 is caused by loss of competent enzyme during the low temperature solvent mixing procedure. In Figure 2, the yield of reactive enzyme is 82%. The average yield over more than 30 preparations was 75 ± 10%.

Simulation of the EPR spectra from samples prepared in the cryosolvent system (Table S1, Figure S2, Supporting Information) yields the same Co^{II}−substrate radical separation distance ($R = 11$ Å) and isotropic electron spin−spin coupling ($J = -300$ MHz) parameters as reported previously for the cryotrapped Co^{II}−substrate radical pair samples in aqueous buffer.[17] The Co^{II}−substrate radical pair line shape is sensitive to changes in R and J.[14,17,18] Therefore, these results provide evidence that the native structure of EAL is maintained in the 41% v/v DMSO/water cryosolvent system.

Arrested Reactivity of the EAL·AdoCbl·Substrate Mixture at 230 K in the Cryosolvent System. The bottom scan in Figure 2 shows that no significant Co^{II}−substrate radical pair accumulates following mixing of a 100-fold excess of (*S*)-2-aminopropanol substrate relative to active sites with EAL holoenzyme in the cryosolvent. The lifetime of the EAL·AdoCbl·substrate ternary complex, with respect to decay to the Co^{II}−substrate radical pair, is $>6.0 \times 10^3$ s at 230 K. A small amount (<1% relative to the Co^{II}−substrate radical pair) of a narrow line width free radical signal at $g = 2.0$ is observed. This unassigned signal is typically observed in Co^{II}−substrate radical pair sample preparations in aqueous solution. The results suggest that the EAL holoenzyme and substrate can be combined in a reaction-arrested state at 230 K. The lifetime is sufficient to allow staging for temperature step studies, which are described in the following section.

Time Dependence of Co^{II}−Substrate Radical Pair Formation Following Temperature Step. The EAL·AdoCbl·substrate mixture prepared at 230 K reacts to form the Co^{II}−substrate radical pair state following a temperature step to higher temperatures. In the temperature range of 234−248 K, the rise of the Co^{II}−substrate radical pair EPR signal is measured by the continuous acquisition of the Co^{II}−radical pair spectrum. To achieve shorter sweep times, only the substrate radical portion of the line shape is acquired. At $T > 248$ K, $\tau_{obs} < 10^2$ s, which is comparable to or less than the instrument dead time of 2.0×10^1 s, and the reaction cannot be monitored by the full spectrum acquisition. At $T < 234$ K, the value of v is <0.3, and poor SNR, especially for early time points, limits certainty in the data. Figure 3 shows a representative data set that was acquired at $T = 242$ K. The peak-to-trough amplitude of the

(43) Babior, B. M.; Moss, T. H.; Orme-Johnson, W. H.; Beinert, H. *J. Biol. Chem.* **1974**, *249*, 4537−4544.
(44) Pilbrow, J. R. In *B12*; Dolphin, D., Ed.; Wiley: New York, 1982; Vol. 1, pp 431−462.
(45) Canfield, J. M.; Warncke, K. *J. Phys. Chem. B* **2005**, *109*, 3053−3046.
(46) Shibata, N.; Masuda, J.; Tobimatsu, T.; Toraya, T.; Suto, K.; Morimoto, Y.; Yasuoka, N. *Structure* **1999**, *7*, 997−1008.
(47) Wetmore, S. D.; Smith, D. M.; Bennett, J. T.; Radom, L. *J. Am. Chem. Soc.* **2002**, *124*, 14054−14065.
(48) Sandala, G. M.; Smith, D. M.; Radom, L. *J. Am. Chem. Soc.* **2005**, *127*, 8856−8864.
(49) Semialjac, M.; Schwarz, H. *J. Org. Chem.* **2003**, *68*, 6967−6983.

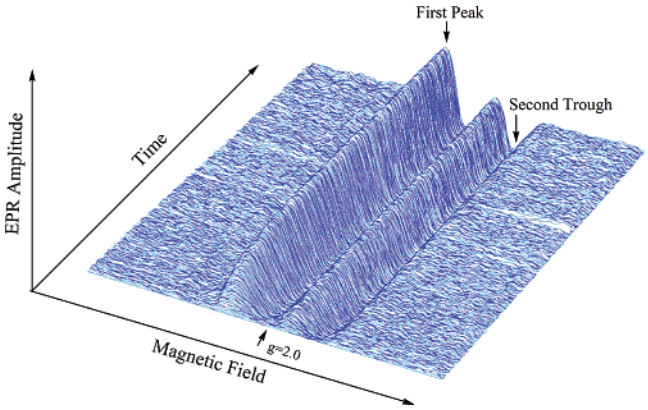

Figure 3. Time dependence of the EPR spectrum of the substrate radical pair state in EAL in the cryosolvent system at $T = 242$ K, following temperature-step initiation of reaction. The time interval between each single-sweep spectrum is 15 s. The free electron resonance position at $g = 2.0$ is shown by the arrow. The first peak and second trough are positioned at 3284 and 3415 G, respectively. The full extents of the magnetic field sweep and time course are 560 G and 6.43×10^3 s, respectively. The concentrations of EAL active sites and coenzyme B_{12} are 150 μM and 15 mM, respectively. EPR conditions: microwave frequency, 9.365 GHz; microwave power, 10 dB (20 mW); magnetic field modulation, 12 G; modulation frequency, 100 kHz; scan rate: 53 G s^{-1}; time constant, 164 ms. The $t = 0$ spectrum (baseline) has been subtracted from each spectrum.

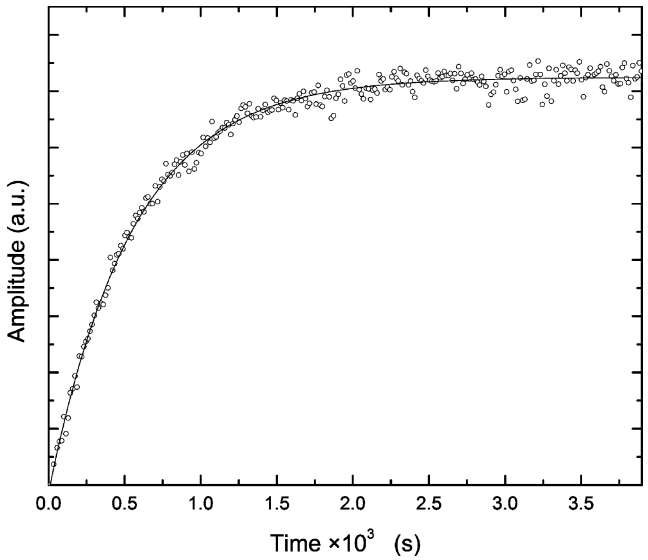

Figure 4. Time-dependence of the EPR amplitude of the substrate radical pair state in EAL in the cryosolvent system at $T = 242$ K, following temperature-jump initiation of reaction. The amplitude is given by the difference between the first peak (3284 G) and second trough (3415 G) amplitudes, as defined in Figure 3. Note that the data are truncated at 3.90×10^3 s, relative to the full time scale of 6.43×10^3 s presented in Figure 3. The experimental data points are overlaid with the best-fit exponential growth function (solid curve; $k_{obs} = 1.82 \times 10^{-3}$ s^{-1}). EPR conditions are as described in the legend to Figure 3.

substrate radical signal in Figure 3 is plotted as a function of time in Figure 4. Note that the data in Figure 4 are truncated at 3.90×10^3 s, relative to the full time scale of 6.43×10^3 s presented in Figure 3, to more clearly display the rise phase of the data. The curve in Figure 4 is well-fit by using a single-exponential growth function with observed first-order rate constant, k_{obs}. The growth of the EPR signal at all temperatures is well-fit by the single-exponential function.

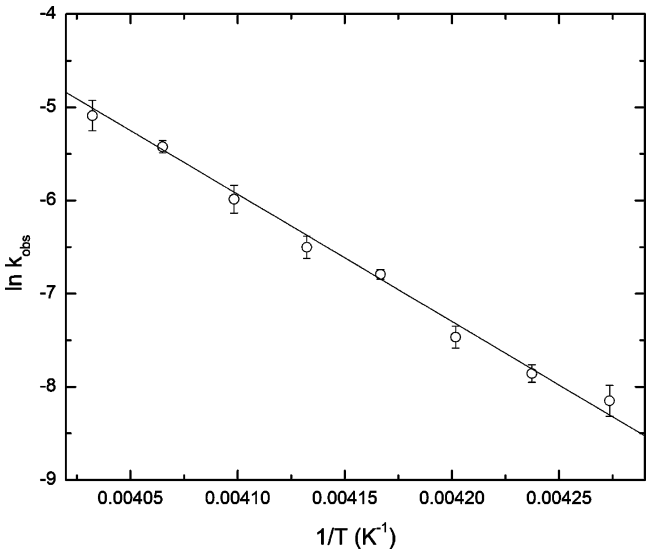

Figure 5. Dependence of the natural logarithm of the observed first-order rate constant for growth of the substrate radical EPR signal on the inverse absolute temperature from $T = 234-248$ K. The substrate/active sites ratio was 100, and the concentration of active sites was 150 μM. The error bars represent the standard deviation obtained by combining three separate measurements at each temperature, which used EAL from three different preparations. Best linear fit (solid line) parameters: slope $= -1.37 \times 10^4$, ordinate intercept $= 5.00 \times 10^1$, $R^2 = 0.993$.

Table 1. Values of the Observed Rate Constant for Co^{II}−Substrate Radical Pair Formation at Different Absolute Temperatures[a]

T (K)	k_{obs} ($\times 10^{-3}$ s^{-1})	
234	0.29	±0.06
236	0.39	±0.04
238	0.58	±0.08
240	1.12	±0.07
242	1.5	±0.2
244	2.5	±0.5
246	4.4	±0.3
248	6.2	±0.9

[a] Values represent the average of at least three separate experiments and the corresponding standard deviation.

Temperature Dependence of k_{obs}. Figure 5 shows the natural logarithm of k_{obs} plotted as a function of inverse absolute temperature, in the Arrhenius plot form. The average values of k_{obs} for the different temperatures, and standard deviations that represent at least three separate determinations, are collected in Table 1. The Arrhenius plot is linear, which suggests that the kinetic mechanism and the rate-limiting step for Co^{II}−substrate radical pair formation are maintained over the temperature range of 234−248 K. As shown below, k_{obs} is a function of at least four microscopic rate constants, and therefore, cannot be used directly to extract A and E_a parameters (or $\Delta G^{\ddagger}$, $\Delta H^{\ddagger}$, and $\Delta S^{\ddagger}$ parameters) that correspond to a single first-order rate constant.

The linear dependence of ln k_{obs} on inverse absolute temperature that is shown in Figure 5 can be extrapolated to obtain an estimated value for k_{obs} at 298 K of 54 s^{-1}. This value is in good agreement with the value of 74 s^{-1} reported for the rate constant for the appearance of cob(II)alamin in the reaction of holo-EAL with (*S*)-2-aminopropanol by using stopped-flow mixing and visible absorption detection.[13] This is evidence that

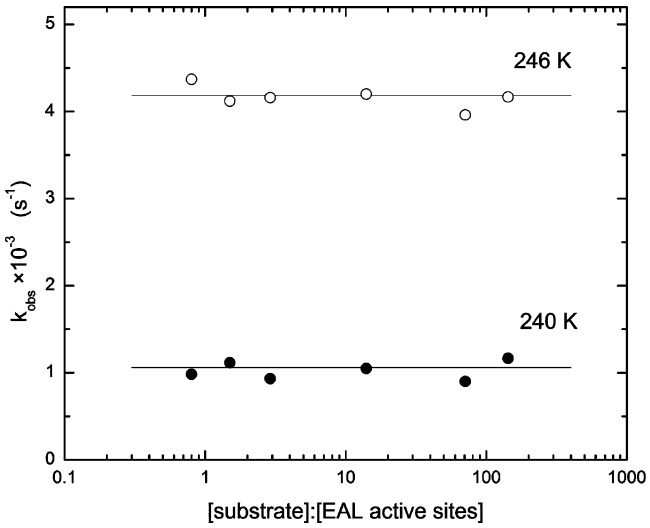

Figure 6. Dependence of the observed first-order rate constant for the growth of the substrate radical pair EPR signal, k_{obs}, on the substrate/active sites ratio at $T = 240$ and 246 K in the cryosolvent system. The lines represent the best zero-slope linear fit to the data. The concentration of EAL active sites was 150 μM.

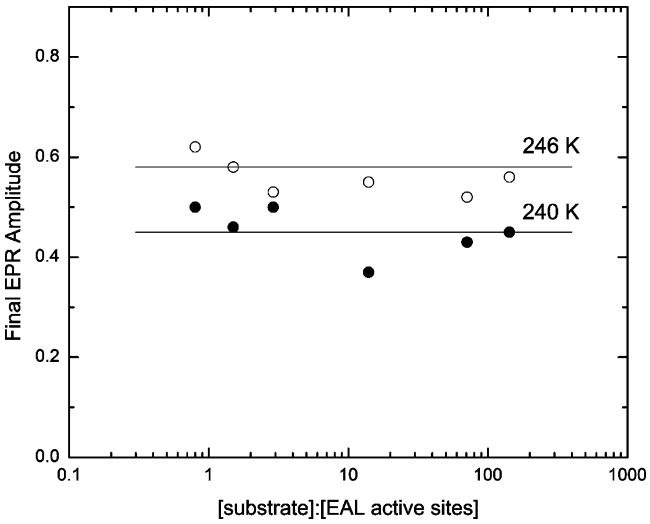

Figure 7. Dependence of the normalized constant (long-time) amplitude of the substrate radical EPR signal on the substrate/active sites ratio at $T =$ 240 and 246 K in the cryosolvent system. The amplitude is normalized as described in the text. The lines represent the best zero-slope linear fit to the data. The concentration of EAL active sites was 150 μM.

the kinetics results obtained at low temperature in the cryosolvent system represent the native enzyme function.

Substrate Concentration Dependence of k_{obs} and the Co^{II}−Substrate Radical Pair Population. Figure 6 shows that k_{obs} is independent of substrate concentration at both 240 and 246 K over the range of substrate/active site ratios, from approximately 1 to 100. Figure 7 shows that the concentration of Co^{II}−substrate radical pair formed at the substrate/active site ratios in Figure 6 is constant, to within ±15%. These results are consistent with the condition, $K_D \ll$ [active sites]. For buffered aqueous solution at 298 K, we have obtained $K_D = 117 \pm 6$ μM for binding of (*S*)-2-aminopropanol to apo-EAL (Anderson, L. E; and Warncke, K., unpublished data). The reported K_M values of 15.5 μM for Clostridium SP[37] and 0.80 μM for *S. typhimurium*[50] also suggest a relatively high affinity of (*S*)-2-aminopropanol for EAL at room temperature in aqueous solution. The significantly lowered temperature in the cryosolvent system would, in principle, decrease the solubility of the positively charged ammonium form of the substrate and decrease the translational entropy contribution to the reactant solution free energy. Both effects would promote tighter binding of substrate to enzyme. Calculations of the ratio of the concentration of substrate-bound enzyme to total enzyme, [ES]/[E_{tot}], performed by using a series of possible K_D values, show that a 10-fold lowering of the room temperature, aqueous phase K_D, to 10 μM in the low-temperature cryosolvent system is consistent with saturation of substrate binding to enzyme active sites over the range of substrate concentrations in Figure 7 (Table S2, Supporting Information).

Figures 6 and 7 provide evidence that the formation of the Co^{II}−substrate radical pair state proceeds from an initial state that is the EAL·AdoCbl·substrate ternary complex. We propose, on the basis of these results, that the mixing of holoenzyme and substrate at 230 K leads to the formation of the ternary complex, and that this state reacts directly to form the Co^{II}−substrate radical pair when the temperature is stepped to higher values. Direct spectroscopic probes of the formation of the ternary complex at 230 K are being pursued.

Equilibrium Approximation for Co^{II}−Substrate Radical Pair Formation. Figures 3 and 4 show that the Co^{II}−substrate radical pair EPR amplitude reaches a constant level at long times ($>5\tau_{obs}$). This is observed at all temperatures in the range of 234−248 K. Furthermore, it was also observed that the Co^{II}−substrate radical pair state formed under the condition, [substrate]/[active site] ≤ 1, was stable on the time scale of the kinetics measurements at each temperature, as observed for the case of excess substrate in Figure 4. This suggests that the rate constant for the rearrangement of the substrate radical to the product radical (step 3 in Figure 1) is significantly smaller than the inverse of the kinetics measurement time. This can be tested by determining the rate constant for decay of the Co^{II}−substrate radical pair at a higher temperature under the condition, [substrate]/[active site] ≤ 1, followed by calculation of the corresponding Arrhenius activation energy, and then by using this activation energy and the Arrhenius rate expression to estimate the rate constant at lower temperatures. The reason for measurements at a higher temperature ($T >$ 250 K) is that a complete decay curve can be obtained. Figure 8 shows the decay for $T = 270$ K. The data in Figure 8 were collected by using the temperature step method[51] of alternately holding the sample at $T = 270$ K for a time interval, and then lowering to $T = 120$ K for EPR spectrum acquisition. The first-order rate constant for the decay (k_{dec}) is 1.5×10^{-3} s^{-1}, which corresponds to an Arrhenius activation energy of 19.3 kcal/mol (from eq 12, with $A = k_B T/h$). This E_a value is consistent with rates reported previously for the optically monitored decay of cob(II)alamin to adenosylcob(III)alamin following substrate depletion at room temperature.[13,41,52] Extrapolation of the Co^{II}−substrate radical decay rate constant to 234−248 K by using the Arrhenius relation with $E_a = 19.3$ kcal/mol gives corresponding values for k_{dec} of 4.6×10^{-6} to 5.1×10^{-5} s^{-1}, respectively. This corresponds to $\tau_{dec} = 2.2 \times 10^5$ s $= 6.0 \times 10^1$ h at 234 K and $\tau_{dec} = 2.0 \times 10^4$ s $= 5.5$ h at 248 K. The

(50) Poyner, R. R.; Anderson, M. A.; Bandarian, V.; Cleland, W. W.; Reed, G. H. *J. Am. Chem. Soc.* **2006**, *128*, 7120−7121.
(51) Lukoyanov, D.; Barney, B. M.; Dean, D. R.; Seefeldt, L. C.; Hoffman, B. M. *Proc. Natl. Acad. Sci. U.S.A.* **2007**, *104*, 1451−1455.
(52) Wallis, O. C.; Bray, R. C.; Gutteridge, S.; Hollaway, M. R. *Eur. J. Biochem.* **1982**, *125*, 299−303.

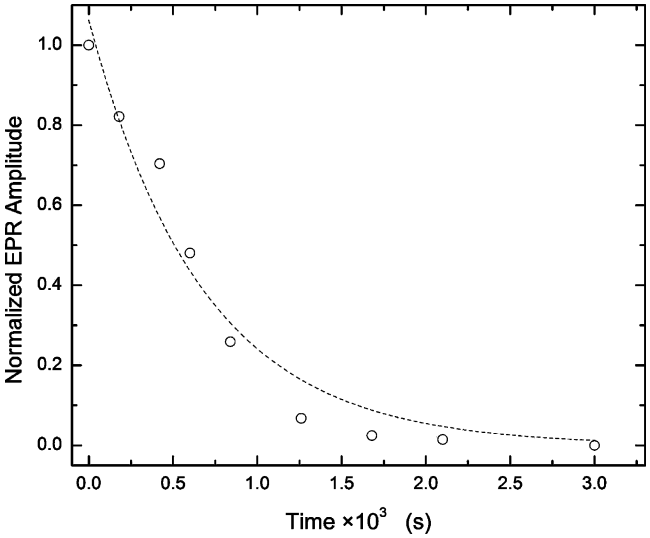

Figure 8. Time dependence of the decay of the substrate radical EPR amplitude at 270 K in the cryosolvent system under conditions of approximately stoichiometric substrate/active sites. The sample was prepared at 230 K and temperature-stepped to 270 K to initiate the reaction. The sample temperature was then alternately held at 270 K for the indicated time intervals and lowered to 120 K for EPR spectrum acquisition. The sample contained 160 μM substrate and 180 μM active sites. The amplitude is normalized to the initial amplitude following the temperature jump to 270 K. The dashed curve shows the fit of a monoexponential decay function to the data ($k_{dec} = 1.49 \times 10^{-3}$ s^{-1}).

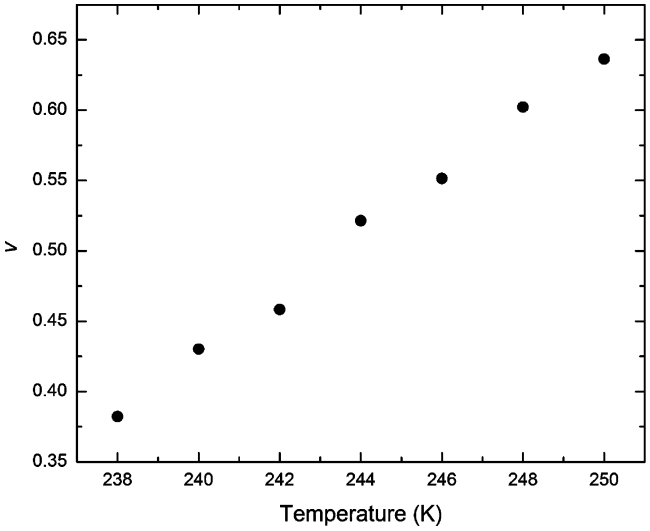

Figure 9. Normalized equilibrium saturation of the substrate radical EPR amplitude as a function of absolute temperature. The results for a single sample are shown, with the nonmonotonic sequence of temperature values as described in the text. The EAL active site and substrate concentrations were 150 μM and 15 mM, respectively.

value of τ_{dec}/τ_{obs} is therefore $\sim 10^2$ over the temperature range, which indicates that the rate of rearrangement of substrate radical to product radical is negligible on the time scale of Co^{II}−substrate radical formation. Therefore, we approximate the reaction of the ternary complex to form the Co^{II}−substrate radical pair as a relaxation to equilibrium.

Equilibrium Perturbation by Temperature Step. The influence of temperature on the proposed equilibrium between the ternary complex and the Co^{II}−substrate radical pair state was addressed by temperature-step perturbation under conditions of excess substrate relative to active sites. A single sample was used in each of three separate experiments. Figure 9 shows the normalized substrate radical amplitude, v, as a function of temperature (additional data is presented in Figure S3, Supporting Information). The amplitude is normalized by using the amplitude of the substrate radical signal obtained after warming the sample to 273 K, followed by 5-min incubation at this temperature (eq 1). In Figure 9, the applied temperature perturbation sequence was not linear to determine if the observed changes in the EPR amplitude of the Co^{II}−substrate radical pair were reversible. The sequence of temperature changes is as follows: 238 → 242, 242 → 240, 240 → 246, 246 → 244, 244 → 250, and 250 → 248 K. The linear trend in Figure 9 indicates a reversible, temperature-dependent equilibrium between the ternary complex and the Co^{II}−substrate radical pair state. The value of v increases with increasing temperature from 0.37 to 0.64. Therefore, the ternary complex and the Co^{II}−substrate radical pair have comparable stabilities over the temperature range, with a trend toward a more stable Co^{II}−substrate radical pair state as temperature increases.

Attempted Detection of Paramagnetic Intermediate States. The presence of paramagnetic intermediate states, and in particular the Co^{II}−5′-deoxyadenosyl radical pair, was addressed by using EPR spectroscopy of the reacting system at 234−248 K. Figure 10 shows normalized EPR spectra for $T = 242$ K that represent the average of blocks (sets) of spectra that were obtained at the midpoint of the rise of the Co^{II}−substrate radical pair signal (Figure 10A), and in the equilibrium state following the rise (Figure 10B). The block averaging improves the SNR of individual spectra obtained from the small volume, 2-mm outer diameter capillary tubes used in the liquid-state experiments. The two spectra in Figure 10 are identical, and they do not differ significantly from the control aqueous solution spectrum of the substrate radical shown in Figure 2. The results presented in Figure 10, and those of similar experiments performed at different temperatures over the range of 234−248 K, show that no paramagnetic species, other than the Co^{II}−substrate radical pair, are detectable in spectra obtained under pre-equilibrium or equilibrium conditions in the cryosolvent system at SNR ≤ 50.

In a second, higher sensitivity approach to detecting paramagnetic intermediates, anaerobic samples of the equilibrated system were prepared, and the sample temperature was rapidly lowered to 77 K by immersion in liquid nitrogen. EPR spectra were then acquired for the samples at 6 K with extended signal averaging, and SNR = 1300 for the substrate radical signal was achieved. No EPR signals, other than the EPR signal from the Co^{II}−substrate radical pair, were observed. A representative spectrum for a sample equilibrated at 242 K is presented in Figure 11. Expanding the range of the magnetic field sweep to 50−5000 G, which would include the region of the "half-field transition" for strongly coupled radical pairs,[14,53] also did not reveal EPR signals attributable to additional EAL-associated paramagnetic species. Therefore, the Co^{II}−substrate radical pair EPR spectrum is the only EPR spectrum that is detected at SNR = 1300 in cryotrapped samples at 6 K.

Discussion

Kinetic Model for Reaction of the Ternary Complex To Form the Co^{II}−Substrate Radical Pair. Scheme 3 shows the

(53) Atherton, N. M. *Principles of Electron Spin Resonance;* Ellis Horwood: New York, 1993.

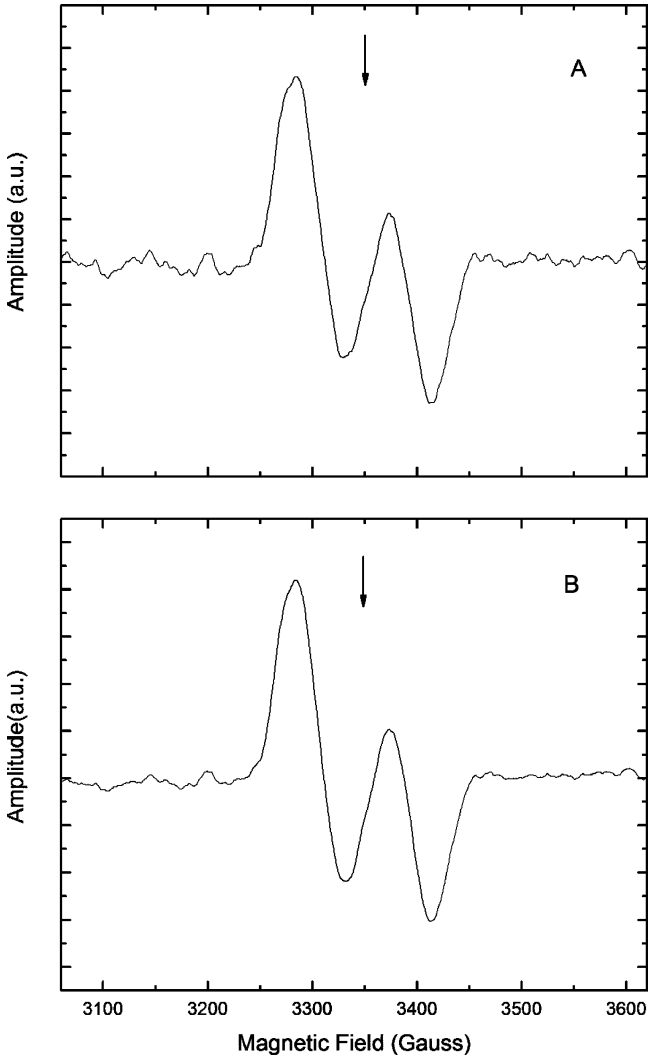

Figure 10. Block-averaged EPR spectra of the substrate radical obtained during reaction at $T = 242$ K. The free electron resonance position at $g = 2.0$ is shown by the arrow. (A) Spectrum representing the midpoint of the rise of the substrate radical EPR signal, obtained over 40−80% of the final amplitude (18 spectra averaged). (B) Spectrum representing the equilibrium state (constant amplitude) of the substrate radical EPR signal (100 spectra averaged). The substrate and EAL active site concentrations were 150 μM and 15 mM, respectively. EPR conditions: microwave frequency, 9.365 GHz; microwave power, 10 dB (20 mW); magnetic field modulation, 12 G peak−peak; modulation frequency, 100 kHz; field sweep rate, 53 G s^{-1}; time constant, 164 ms.

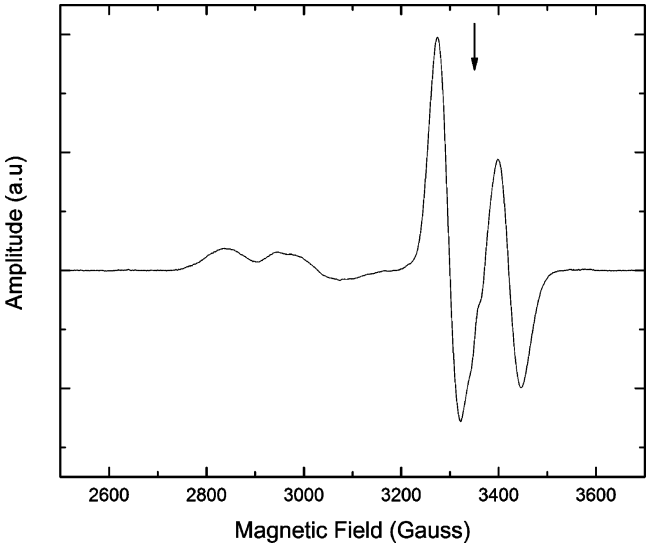

Figure 11. EPR spectrum of the cryotrapped substrate radical after equilibration at $T = 242$ K, acquired at $T = 6$ K. The free electron resonance position at $g = 2.0$ is shown by the arrow. The substrate and EAL active site concentrations were 7.5 mM and 150 μM, respectively. EPR conditions: microwave frequency, 9.378 GHz; microwave power, 30 dB (0.2 mW); magnetic field modulation, 10 G peak−peak; modulation frequency, 100 kHz; field sweep rate, 3.7 G s^{-1}; time constant, 164 ms; average of eight spectra, minus baseline.

linear two-step, three-state kinetic mechanism that we propose for the observed reaction of the EAL·AdoCbl·substrate ternary complex to form the Co^{II}−substrate radical pair. The mechanism corresponds to steps 1 and 2 in the catalytic cycle presented in Figure 1. The states, A_1, A_2, and A_3, in Scheme 3 represent, in compact notation, the ternary complex, the Co^{II}−5′-deoxyadenosyl radical pair, and the Co^{II}−substrate radical pair, respectively. The identification of A_1 as the ternary complex is based on the substrate concentration-independence of both k_{obs} and the amplitude of the Co^{II}−substrate radical pair, as shown in Figures 6 and 7. These results indicate that the condition, $K_D \ll$ [active sites], holds for the interaction of EAL and substrate. A third step, which represents the conversion of substrate radical to product radical (step 3 in Figure 1) is not included in the mechanism, because the level of Co^{II}−substrate radical pair state is constant for a long period of time (Figures 3 and 4), and the decay rate, calculated on the basis of the E_a value for the decay obtained at 270 K (Figure 8), implies that the rate of substrate radical decay through conversion to the product radical is $\sim 10^2$-fold less than k_{obs} over the temperature range, 234−248 K. In the following analysis, eqs 3−11 for the two-step mechanism are used to describe the time dependence and equilibrium populations of the A_i states.

Relations among Experimental Observables and Microscopic Rate Constants. In the following, expressions are derived from the mechanism in Scheme 3 and the experimental constraints, which show that the equilibrium constants that link the A_i strongly disfavor formation of the A_2 state. This accounts for the observed monoexponential growth of the Co^{II}−substrate radical pair EPR signal. The general linear two-step mechanism predicts a biexponential growth of A_3 (the Co^{II}−substrate radical pair) as expressed by eqs 6 and 7 for the two relaxation constants, λ_2 and λ_3.[42] Paramagnetic signals arising from an intermediate species, A_2 (the Co^{II}−5′-deoxyadenosyl radical pair), were detected neither in the kinetic experiments at 234−248 K, nor in samples at equilibrium that were cryotrapped and examined by EPR spectroscopy at 6 K (Figures 10 and 11). The highest SNR achieved was 1300. Therefore, if it is assumed that the Co^{II}−substrate radical pair and putative Co^{II}−5′-deoxyadenosyl radical pair EPR signals have comparable derivative amplitudes, then the SNR > 10^3 leads to the inequality, $([A_2]_\infty)/([A_3]_\infty) < 10^{-3}$. This implies that $K_{23} > 10^3$. Furthermore, the equilibrium perturbation results presented in Figures 9 and S3 show that $\nu \approx 0.5$ over the temperature range examined, which implies that $([A_3]_\infty)/([A_1]_0) \approx 0.5$ (eq 11). Substitution of the condition, $[A_2]_\infty < 10^{-3}[A_3]_\infty$, into eq 8 leads to the simplified expression, $[A_1]_0 = [A_1]_\infty + [A_3]_\infty$. Substitution of this simplified expression into eq 11, and rearrangement, leads to the approximation, $([A_3]_\infty)/([A_1]_\infty) \approx 1$, which holds over the temperature range examined. Substitution of this result and $K_{23} > 10^3$ (from above) into eq 10 leads to the inequality, $K_{12} <$

10^{-3}. The limiting values obtained for K_{12} ($= k_{12}/k_{21}$) and K_{23} ($= k_{23}/k_{32}$) indicate that the following inequalities hold for the corresponding pairs of rate constants:

$$k_{32} < 10^{-3} k_{23} \tag{14}$$

$$k_{12} < 10^{-3} k_{21} \tag{15}$$

The substitution of the limits from eqs 14 and 15 into eqs 6 and 7 leads to the following simplified approximate relations between λ_2 and λ_3 and the microscopic rate constants:

$$\lambda_2 = k_{21} + k_{23} \tag{16}$$

$$\lambda_3 = \frac{k_{12}k_{23} + k_{21}k_{32}}{k_{21} + k_{23}} \tag{17}$$

From the comparison of the right-hand sides of eqs 16 and 17 with the inequalities in eqs 14 and 15, $\lambda_2 > 10^3\ \lambda_3$. The relaxation represented by λ_2 will therefore not be detectable at our time resolution, and the growth of A_3 (the state that corresponds to the EPR-detected Co^{II}−substrate radical pair) will be governed by an apparent monoexponential process, which is in accord with experiment. The time dependence of the growth of the normalized concentration of A_3 is expressed as follows:

$$\frac{[A_3]_t}{[A_1]_0} \approx \frac{[A_3]_\infty}{[A_1]_0}(1 - e^{-\lambda_3 t}) \tag{18}$$

The parameters in eq 18, $([A_3]_\infty)/([A_1]_0)$ and λ_3, are related to the experimental observables, k_{obs} and υ, as follows:

$$k_{obs} = \lambda_3 = \frac{k_{12}k_{23} + k_{21}k_{32}}{k_{21} + k_{23}} \tag{19}$$

$$\upsilon = \frac{[A_3]_\infty}{[A_1]_0} = \frac{k_{12}k_{23}}{k_{12}k_{23} + k_{21}k_{32}} \tag{20}$$

The system is underdetermined, with respect to obtaining the values of the k_{ij}.

Relative Free Energy of the Co^{II}−5′-Deoxyadenosyl Radical Pair Intermediate State. The limiting values of K_{12} and K_{23} allow an estimation of the free energy of the Co^{II}−5′-deoxyadenosyl radical pair state for the temperature range, 234−248 K. The inequalities, $K_{12} < 10^{-3}$ and $K_{23} > 10^3$, imply that $\Delta G_{12} > 3.3$ kcal/mol and $\Delta G_{23} < -3.3$ kcal/mol, respectively, over the range of temperatures examined. The limiting values for ΔG_{12} and ΔG_{23} indicate that the free energy of the Co^{II}−5′-deoxyadenosyl radical pair state is >3.3 kcal/mol, relative to the ternary complex and Co^{II}−substrate radical pair states.

Thermodynamics of Co^{II}−Substrate Radical Pair State Formation. The thermodynamic parameters, ΔG_{13}, ΔH_{13}, and ΔS_{13}, for the transition from the A_1 (ternary complex) state to the A_3 (Co^{II}−substrate radical pair) state were determined by van't Hoff analysis of K_{13} (eq 13). Values of K_{13} at different temperatures were obtained from the corresponding υ values by using the following expression:

$$K_{13} = \frac{\upsilon}{1 - \upsilon} \tag{21}$$

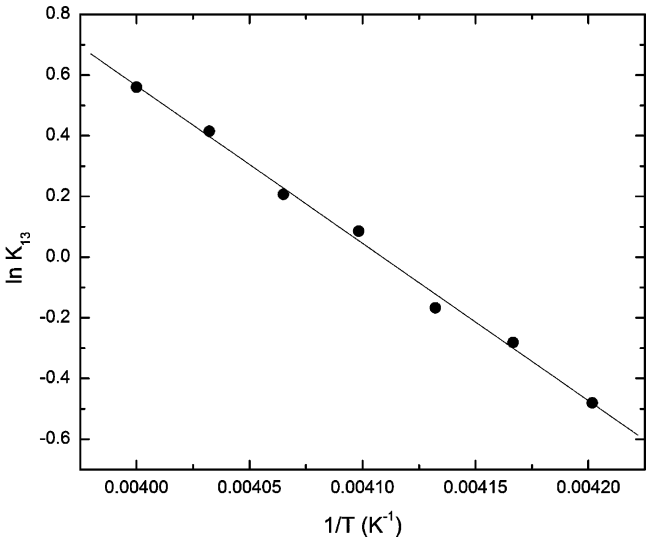

Figure 12. Van't Hoff plot of the equilibrium constant, K_{13}, representing the equilibrium between the ternary complex (state A_1) and the Co^{II}−substrate radical pair (state A_3), over the temperature range of 238−250 K. Best linear fit (solid line) parameters: slope $= -5.19 \times 10^3$, ordinate intercept $= 2.13 \times 10^1$, $R^2 = 0.995$.

Equation 21 was derived by dividing the numerator and denominator of the right-hand side of eq 20 by $k_{21}k_{23}$, expressing the resulting ratio of rate constants as $K_{12}K_{23} = K_{13}$, and rearranging to express K_{13} in terms of υ. Figure 12 shows the van't Hoff plot for K_{13} that was obtained by using the υ values presented in Figure 9. Two additional van't Hoff plots from separate experiments are shown in Figure S4 (Supporting Information). Table 2 presents values of ΔH_{13} (10.8 ± 0.8 kcal/mol) and ΔS_{13} (45 ± 3 cal/mol/K) that were obtained from the average of the linear fit parameters from each van't Hoff plot. Values of ΔG_{13} were calculated from the Gibbs expression ($\Delta G = \Delta H - T\Delta S$). The value of ΔG_{13} is zero over the temperature range, to within the standard deviation of the measurements (+0.1 ± 1.1 kcal/mol at 238 K to −0.5 ± 1.1 kcal/mol at 250 K). The free energy contributions of the enthalpy and entropy ($T\Delta S_{13} = -10.7$ to -11.3 kcal/mol for 238 to 250 K, respectively) are comparable. Coenzyme B_{12}-dependent RTPR also establishes an equivalent free energy at ambient temperature between the dGTP activator-bound enzyme and the first metastable Co^{II}−radical (thiyl) pair, in the absence of substrate.[19] However, in the substrate-bound condition in EAL, the relative stability of the Co^{II}−radical pair state increases with temperature, and the radical pair state becomes favored over the ternary complex at 298 K by −2.6 kcal/mol, as described below.

EAL protein-associated contributions to the Co^{II}−radical pair stabilization process were estimated by comparison of the experimental parameters in Table 2 with data for the Co−C bond cleavage and hydrogen atom transfer subreactions that are associated with steps 1 and 2 in Figure 1. Solution studies indicate that Co−C bond cleavage, which is involved in the observed $A_1 \rightarrow A_3$ reaction, is associated with a large, unfavorable enthalpy change, ΔH_{Co-C}.[22−24] Comparison of ΔH_{13} with $\Delta H_{Co-C} = 30 \pm 2$ kcal/mol[24] indicates that the unfavorable Co−C bond cleavage is compensated by a favorable enthalpy contribution of approximately −19 ± 2 kcal/ mol in EAL. The favorable enthalpy contribution to the $A_1 \rightarrow A_3$ process in EAL originates, in part, from the linkage of Co−C bond cleavage to the first hydrogen atom transfer reaction, HT1 (Figure 1). The

Table 2. Values of Experimentally Determined Thermodynamic Parameters for the A_1 (Ternary Complex)$-A_3$ (Co^{II}−Substrate Radical Pair) Equilibrium in the Cryosolvent System, and Estimated EAL Protein-Associated Contributions

reaction	ΔG^b (kcal/mol)		ΔH (kcal/mol)		ΔS (cal/mol/K)	
overall, 1 → 3	0.0	±1.1	10.8	±0.8	45	±3
EAL contribution,[a] 1 → 3	−24	±3	−13	±3	38	±3

[a] Estimated by using eq 22, with $\Delta H_{Co-C} = 30 \pm 2$ kcal/mol,[24] $[\Delta H_{C1-H} - \Delta H_{C5'-H}] = -6 \pm 2$ kcal/mol,[43,49−51] $\Delta S_{Co-C} = 7$ cal/mol/K,[24] and $\Delta S_{HT} = 0$, as described in the text. [b] Free energy calculated for 240 K.

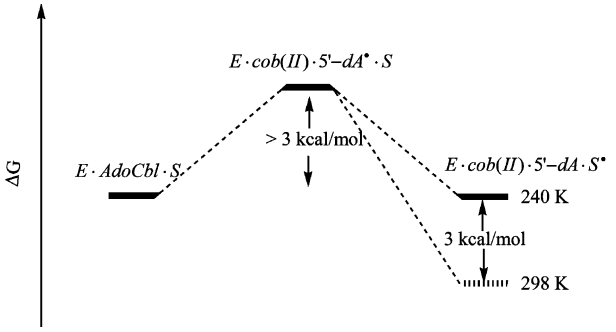

Figure 13. Schematic free energy diagram of the relative free energy levels of the ternary complex (state A_1), Co^{II}−5′-deoxyadenosyl radical pair (state A_2), and Co^{II}−substrate radical pair (state A_3) in EAL. The relative free energy levels for $T = 240$ K were directly determined by experiment, and the change at $T = 298$ K was obtained by extrapolation of data for $T = 236-250$ K. The change in free energy between the ternary complex and Co^{II}−substrate radical pair states at $T = 298$ K and $T = 240$ K is referenced to the level of the ternary complex.

contributions of covalent bond-making and bond-breaking processes to ΔH_{13} are estimated by using the following expression:

$$\Delta H_{bond} \approx \Delta H_{Co-C} + \Delta H_{C1-H} - \Delta H_{C5'-H} \qquad (22)$$

where ΔH_{C1-H} and $\Delta H_{C5'-H}$ represent the enthalpy for hydrogen atom abstraction from C1 and C5′, respectively. The value of $[\Delta H_{C1-H} - \Delta H_{C5'-H}]$ is estimated to be −5 to −7 kcal/mol, based on the experimental C−H bond dissociation energies reported for ethanol and ethane.[54,55] The value of −5 to −7 kcal/mol arises from the larger (more favorable) resonance stabilization energy associated with the formation of the α-hydroxy-stabilized[42] radical at C1, relative to the primary alkyl radical at C5′. This estimate of $[\Delta H_{C1-H} - \Delta H_{C5'-H}]$ is in general agreement with values of −6.1 kcal/mol[47] and −6.0 kcal/mol[48] calculated by using ab initio/density functional theory calculations of the energy change associated with hydrogen transfer between 2-ammonium-1-ethanol and the ethanol-1-yl radical in the gas phase, as a simple model for the HT1 step in EAL. Comparable values of −3.2 to −5.7 were obtained by a computational study that included auxiliary groups and additional interactions that contributed to the hydrogen transfer energy.[56] If an average value for $[\Delta H_{C1-H} - \Delta H_{C5'-H}]$ of −6 ± 2 kcal/mol is assumed, then, from eq 22, $\Delta H_{bond} \approx 24 \pm 3$ kcal/mol. The EAL protein-associated contribution to the enthalpy of the $A_1 \rightarrow A_3$ transition is thus approximately equal to $\Delta H_{13} - \Delta H_{bond}$, or -13 ± 3 kcal/mol. In contrast, the residual enthalpy was zero (within the uncertainty) after subtraction of Co−C bond breaking and hydrogen atom exchange contributions to enthalpy of Co^{II}−thiyl radical pair formation, following dGTP activator-induced Co−C bond cleavage in RTPR.[23] We attribute the more favorable protein-associated contribution to the enthalpy of the $A_1 \rightarrow A_3$ transition in EAL to the presence of the bound substrate, which invokes changes in the protein that lead to the "substrate trigger" of cobalt−carbon bond cleavage.

The van't Hoff analysis shows that the $A_1 \rightarrow A_3$ transition in EAL is associated with a relatively large, favorable entropy change of $\Delta S_{13} = 45 \pm 3$ cal/mol/K. In comparison, ΔS_{Co-C} for the Co−C bond cleavage reaction in solution is smaller. A value of $\Delta S_{Co-C} = 7 \pm 1$ cal/mol/K is estimated from the activation entropy for cleavage,[24] under the assumption that the bond re-formation rate process is close to diffusion-controlled.[22,23] If it is assumed that ΔS_{Co-C} is a reasonable estimate of the entropy change for Co−C cleavage contributed by the coenzyme in the enzyme, and that $\Delta S \approx 0$ for the hydrogen atom transfer between carbon donor (C1) and acceptor (C5′) atoms that are at van der Waals contact during reaction,[17,57] then the estimated protein-associated contribution to the $A_1 \rightarrow A_3$ transition is $\Delta S_{13} - \Delta S_{Co-C} \approx 38 \pm 3$ cal/mol/K. A large entropy change of 70 cal/mol/K was determined for the dGTP-activated Co−C bond cleavage and Co^{II}−thiyl radical pair formation in RTPR.[23] Thus, in RTPR, entropic effects dominate the protein-associated contribution to the dGTP-activated Co−C bond cleavage equilibrium.[23] The estimated protein-associated entropic contribution to the free energy change in EAL is −8.9 to −9.4 ± 0.7 kcal/mol from 234 to 248 K, respectively. Therefore, in EAL, the estimated protein-associated enthalpic and entropic contributions to the $A_1 \rightarrow A_3$ transition are comparable.

The thermodynamic parameters for the $A_1 \rightarrow A_3$ transition in EAL, and the estimated EAL protein-associated contributions, are summarized in Table 2. Figure 13 depicts the results of the thermodynamic measurements for low temperature in the cryosolvent system in a schematic free energy profile, including the lower limit on the free energy of the Co^{II}−5′-deoxyadenosyl radical pair state.

Implications for EAL Function under Native Temperature and Solvent Conditions. The ΔH_{13} and ΔS_{13} values in Table 2 and the Gibbs expression lead to an estimated value for ΔG_{13} at 298 K of -2.6 ± 1.2 kcal/mol. Therefore, under physiological conditions, the formation of the Co^{II}−substrate radical pair is predicted to be favored, relative to the ternary complex. The strong protein-associated contributions to both ΔH_{13} and ΔS_{13}

(54) McMillen, D. F.; Golden, D. M. *Annu. Rev. Phys. Chem.* **1982**, *33*, 493−532.
(55) Berkowitz, J.; Ellison, G. B.; Gutman, D. *J. Phys. Chem.* **1994**, *98*, 2744−2765.
(56) Semialjac, M.; Schwarz, H. *Chem.−Eur. J.* **2004**, *10*, 2781−2788.
(57) Warncke, K.; Utada, A. S. *J. Am. Chem. Soc.* **2001**, *123*, 8564−8572.
(58) Carty, T. J.; Babior, B. M.; Abeles, R. H. *J. Biol. Chem.* **1971**, *246*, 6313−6317.
(59) Graves, S. W.; Fox, J. A.; Babior, B. M. *Biochemistry* **1980**, *19*, 3630−3633.
(60) Ke, S.-C.; Torrent, M.; Museav, D. G.; Morokuma, K.; Warncke, K. *Biochemistry* **1999**, *38*, 12681−12689.
(61) Abend, A.; Bandarian, V.; Nitsche, R.; Stupperich, E.; Retey, J.; Reed, G. H. *Arch. Biochem. Biophys.* **1999**, *370*, 138−141.

are essential for the thermodynamic biasing of the native reaction in the forward direction of Co−C bond cleavage and Co^{II}−substrate radical pair formation.

Acknowledgment. This work was supported by NIH Grant DK54514. The purchase of the Bruker E500 EPR spectrometer was funded by NIH NCRR Grant RR17767 and by Emory University.

Supporting Information Available: Overlay of amplitude-normalized EPR spectra for Co^{II}−substrate radical pair in water and cryosolvent, EPR simulation of Co^{II}−substrate radical pair EPR spectrum, two additional υ versus T data sets, and two additional van't Hoff plots. This material is available free of charge via the Internet at http://pubs.acs.org.

JA710069Y